Talanta 115 (2013) 718–723

Contents lists available at SciVerse ScienceDirect

Talanta

journal homepage: www.elsevier.com/locate/talanta

Photoluminescent C-dots@RGO for sensitive detection of hydrogen peroxide and glucose

Ting-Yin Yeh, Chen-I Wang, Huan-Tsung Chang *

Department of Chemistry, National Taiwan University, 1, Section 4, Roosevelt Road, Taipei, Taiwan

ARTICLE INFO

Article history:
Received 2 May 2013
Received in revised form
20 June 2013
Accepted 21 June 2013
Available online 28 June 2013

Keywords:
Photoluminescent
C-dots
Reduced graphene oxide
Hydrogen peroxide
Glucose

ABSTRACT

We have demonstrated sensitive detections of hydrogen peroxide (H_2O_2) and glucose using reduced graphene oxide decorated with carbon dots (C-dots@RGO). The C-dots@RGO prepared from catechin (reducing agent and carbon source) and graphene oxide via hydrothermal routes possesses excitation-wavelength-dependence photoluminescence (PL) characteristics, with maximum excitation and emission wavelengths of 365 and 440 nm, respectively. The C-dots@RGO is stable in solution containing NaCl up to 350 mM, but is quenched by reactive oxygen species (ROS). ROS reacts with H_2O_2 and thus its PL quenching toward the C-dots@RGO is minimized. When using C-dots@RGO and glucose oxidase (GO*x*), the PL assay allows detection of glucose in the presence of 10 μM of bovine serum albumin, with linearity over a concentration range from 1 to 60 μM ($r=0.99$) and a limit of detection (at a signal-to-noise ratio of 3) of 140 nM. The practicality of this assay has been validated by determining the concentrations of glucose in serum and saliva samples, with results of 5.1 ± 0.6 mM ($n=3$) and 117.9 ± 8.1 μM ($n=3$), respectively. Our simple and sensitive assay opens a new avenue of developing assays for various analytes using C-dots@RGO in conjunction with different enzymes.

1. Introduction

Diabetes has affected billions of people in the world and is one of the most important public-health issues [1]. Monitoring of blood glucose levels is extremely essential, mainly because dysfunction of glucose uptake caused by insulin deficiency or resistance is associated with diabetes [2]. The blood glucose concentrations in healthy people and diabetic patients are in the ranges of 3–8 and 9–40 mM, respectively [3]. To provide sensitivity and selectivity, most commercial sensors take advantage of high chemical activity of H_2O_2 that is a product of a specific reaction between glucose and glucose oxidase (GO*x*) in the presence of O_2 [3]. Amperometric sensors are considered to be the most popular in the market, while they all have limited lifetimes (mostly less than 7 days) [4,5].

A number of optical based sensors for the detection of glucose have been demonstrated [6–9]. Like electrochemical based sensors, absorption, chemiluminescence, and fluorescence based sensors all take the advantage of the strong oxidizing strength of H_2O_2 for conversion of substrates to optically active products [10,11]. Common substrates for H_2O_2 in the absorption, chemiluminescence, and fluorescence detection modes are 2,2′-azino-bis (3-ethylbenzothiazoline-6-sulfonic acid), luminol, and dihydrorhodamine 123, respectively [12–14]. Although these sensors provide advantages of sensitivity, rapidity, and/or specificity, expensive substrates are required and sometimes matrix interference occurs. Thus, reliable, sensitive, and cost-effective approaches for the detection of H_2O_2 and glucose are still needed.

Nanoparticles have become popular for the detection of H_2O_2 and glucose [15–21]. Alternatively, luminescent gold nanodots have been used for the detection of H_2O_2 and glucose with limits of detection (LODs) of 30 nM and 1.0 μM, respectively, at a signal-to-noise (*S*/*N*) ratio of 3 [9]. However, use of expensive gold ions, poor photostability, and instability of gold nanodots in the presence of high salt (e.g. > 20 mM NaCl) are problematic [22]. Enzyme mimics of Fe_3O_4 magnetic NPs and FeTe nanorods in conjunction with GO*x* are interesting approaches to the detection of glucose [8,19]. However, optical substrates are still required for these techniques.

Recently, we have demonstrated preparation of photoluminescent carbon nanodots (C-dots) from used tea, used coffee grounds, and inexpensive small organic compounds through hydrothermal routes [23,24]. The formation of C-dots is believed to occur through a mechanism involving sequential dehydration, polymerization, carbonization, and passivation. The emission wavelengths of C-dots cover a broad wavelength range (from 300 to 700 nm), which are dependent on the excitation wavelength [25]. The interesting optical property is due to crystal defects and existence

* Correspondence auothor. Tel./fax: +886 2 33661171.
E-mail address: changht@ntu.edu.tw.(H.-T. Chang)

0039-9140/$ - see front matter © 2013 Elsevier B.V. All rights reserved.
http://dx.doi.org/10.1016/j.talanta.2013.06.035

of many different sizes of C-dots [26]. Very recently, we have prepared reduced graphene oxide decorated with carbon dots (C-dots@RGO) from catechin and graphene oxide (GO) through a hydrothermal reaction [27]. Graphene and its derivatives are attractive materials for sensing, mainly because of their unique two-dimensional (2D) structures with large surface area and unique electronic and physicochemical properties [28]. Like C-dots, the C-dots@RGO is highly water soluble, photostable, and chemical stable (up to 500 mM NaCl). The photoluminescence (PL) of C-dots and C-dots@RGO is quenched by reactive oxygen species (ROS) [27]. Based on the generation of ROS by H_2O_2, they both can be used for the detection of H_2O_2; the C-dots@RGO exhibits higher sensitivity for H_2O_2 than pure C-dots, mainly because of its higher ROS generation efficiency [27].

In this work, we used C-dots@RGO for the detection of H_2O_2 based on its reaction with ROS that led to decreases in ROS induced quenching. This new approach for the detection of H_2O_2 is through a "turn on" process, which is different from our previous "turn off" PL approach [27]. Herein, we demonstrated an alternative "turn on" PL approach based on photoluminescent C-dots@RGO for highly sensitive detection of H_2O_2 and glucose. When compared to the "turn off" PL approach, C-dots@RGO reacts directly with H_2O_2 at a rapid rate when using the "turn on" approach. In addition, H_2O_2 is relatively more stable and it has longer half-life than ROS, which leads to highly reproducible and stable signals. This assay provides advantages of sensitivity, rapidity, and specificity for H_2O_2 and glucose. Moreover, the sensitivity of H_2O_2 detection was greatly improved in the presence of bovine serum albumin (BSA), revealing that this probe has great potential to be used for the quantitative detection of H_2O_2 in biological samples. The C-dots@RGO itself and combined with GO*x* were used to determine the concentrations of H_2O_2 and glucose, respectively. We validated the low-cost, sensitive, and selective sensing system for the determination of the concentrations of glucose in blood and saliva samples, with high accuracy and precision.

2. Material and methods

2.1. Chemicals

BSA, catechin hydrate, cysteine, disodium hydrogen phosphate, fructose, galactose, globulin from chicken egg white, glucose, glutathione, GO*x*, homocysteine, human serum albumin (HSA), H_2O_2 (15 M), lactose, maltose, mannose, monopotassium phosphate, potassium chloride, sodium chloride, and sodium citrate dehydrate were purchased from Sigma-Aldrich (St. Louis, MO, USA). Ethylenediaminetetraacetic acid (EDTA), and monobasic, dibasic and tribasic sodium phosphates were purchased from Acros Organics (Milwaukee, WI, USA). Commercially available GO dispersion in water (5 mg mL^{-1}) was obtained from Graphene Supermarket (Calverton, NY, USA). Ammonium hydroxide solution (8.83 M) was purchased from Fisher Scientific (Loughborough, Leicestershire, UK). Ultrapure water (18.2 MΩ cm^{-1}) from a Milli-Q ultrapure system was used in this study.

2.2. Synthesis of C-dots@RGO

C-dots@RGO was prepared through a hydrothermal route according to our previous approach [27]. Briefly, 21.6 mg catechin hydrate was dissolved in 6.5 mL ultrapure water, in which GO (5 mg mL^{-1}, 0.5 mL) and concentrated ammonium hydroxide (8.83 M, l.0 mL) solutions were added to. The mixture was heated in a stainless steel autoclave at 300 °C for 2 h. After annealing, the C-dots@RGO was subjected to several cycles of filtration to remove free C-dots, matrix, and large particles. The concentration of C-dots@RGO in the final filtrate was represented as 1.0 × (ca. 0.2 mg mL^{-1}) and kept at 4 °C prior to use.

2.3. Characterization of C-dots@RGO

A Cintra 10e double-beam UV–vis spectrophotometer (GBC, Victoria, Australia) was used to record the absorption (extinction) of the as-prepared C-dots@RGO solution. The morphology of the as-prepared C-dots@RGO was recorded by transmission electron microscopy (TEM) (H7100, Hitachi High-Technologies Corporation, Tokyo, Japan). The PL spectra of C-dots@RGO were recorded using a Cary Eclipse fluorescence spectrophotometer (Varian, Palo Alto, CA, USA).

2.4. Blood and saliva sampling

The whole blood and serum samples used in this study were collected from healthy volunteer donors (25-year-old males). Each of the blood samples (6 mL) was taken from cubital vein in the early morning after overnight fasting (at least 8 h) [29]. The whole blood samples were collected immediately into glass vials containing 4% sodium citrate prepared in phosphate buffered saline (PBS; pH 7.4, containing 137 mM NaCl, 2.7 mM KCl, 10 mM Na_2HPO_4, and 2.0 mM KH_2PO_4) to prevent pore clogging. Each of the blood samples was separately mixed with sodium citrate, with a volume ratio of 9/1. To each of the blood samples, EDTA aqueous solution (8%, 0.15 mL) was added. After immediate centrifugation (1789 g, 10 min, 4 °C), each of the supernatants (sera) was transferred to a polypropylene test tube. The sera were stored at −20 °C before analysis.

The saliva samples were collected from healthy volunteers (25-year-old males) within a period of 5 min upon waking in the morning. Prior to collection of the samples, they were asked to avoid any oral activities (drinking, eating, smoking, tooth brushing, etc.). Each of the saliva samples (1.0 mL) was collected into a plastic tube in the unstimulated state [30,31], which was immediately centrifuged (7500 g, 15 min, 4 °C). Each of the supernatants was transferred to another vial and stored at −20 °C before analysis.

2.5. Detection of H_2O_2 and glucose in standard solutions

To optimize pH, aliquots of H_2O_2 (1.5 mM, 30 μL) were separately added to sodium phosphate solutions (22 mM, pH 4.0–11.0, 270 μL) containing C-dots@RGO (0.11 ×). The solutions were equilibrated at 25 °C for 5 min. The NaCl concentration was optimized by equilibrating aliquots of sodium phosphate solutions (22 mM, pH 9.0, 270 μL) containing glucose (111.1 μM), GO*x* (1.1 μM), and NaCl (0–388.9 mM) at 37 °C for 5 min, followed by the addition of C-dots@RGO (1 ×, 30 μL). The solutions were equilibrated at 25 °C for 5 min. To determine the optimal pH for the detection of glucose, aliquots of sodium phosphate solutions (22 mM, pH 4.0–11.0, 270 μL) containing GO*x* (1.1 μM) and glucose (111.1 μM) were equilibrated at 37 °C for 5 min, followed by the addition of C-dots@RGO (1 ×, 30 μL). The concentration of GO*x*, was optimized by equilibrating aliquots of sodium phosphate solutions (22 mM, pH 9.0, 270 μL) containing glucose (111.1 μM), and GO*x* (0.1–11.1 μM) at 37 °C for 5 min, followed by the addition of C-dots@RGO (1 ×, 30 μL). The solutions were equilibrated at 25 °C for 5 min. We tested the effect of BSA on the detection of glucose through equilibrating aliquots of sodium phosphate solutions (22 mM, pH 9.0, 270 μL) containing glucose (1.1–66.7 μM), GO*x* (1.1 μM), and BSA (1.1 or 11.1 μM) at 37 °C for 5 min, followed by the addition of C-dots@RGO (1 ×, 30 μL). The mixtures were equilibrated at 25 °C for 5 min. The PL values of C-dots@RGO

(0.1 ×) in sodium phosphate solutions (20 mM, pH 9.0, 300 μL) containing various concentrations of BSA (1.1–55.6 μM) that had been equilibrated at 25 °C for 5 min were recorded to evaluate the effect of BSA on the PL of C-dots@RGO. For quantitative detection of H_2O_2, aliquots of sodium phosphate solutions (20 mM, pH 9.0, 300 μL) containing H_2O_2 (0–150 μM) and C-dots@RGO (0.1 ×) were equilibrated at 25 °C for 5 min. For quantitative detection of glucose, aliquots of sodium phosphate solution (22 mM, pH 9.0, 270 μL) containing glucose (0–44.4 μM,) and GO*x* (1.1 μM) were equilibrated under gentle shaking at 37 °C for 5 min. Subsequently, each of the mixtures was separately mixed with C-dots@RGO solution (1 ×, 30 μL). The solutions were then equilibrated at 25 °C for 5 min before PL measurement. The specificity of the present assay for glucose over other tested carbohydrates was evaluated by recording the PL values of C-dots@RGO in sodium phosphate solution (20 mM, pH 9.0, 300 μL) containing glucose (100 μM), GO*x* (1.0 μM), and any one (100 μM) of the following carbohydrates: maltose, fructose, lactose, galactose, and mannose. To study the effect of proteins on the detection of glucose, BSA and globulin (100 μM, 30 μL) were separately added to aliquots of sodium phosphate solutions (25 mM, pH 9.0, 240 μL) containing glucose (125 μM) and GO*x* (1.3 μM). On the other hand, cysteine, homocysteine, and glutathione (100 μM, 30 μL) were separately added to aliquots of sodium phosphate solutions (25 mM, pH 9.0, 240 μL) containing glucose (125 μM) and GO*x* (1.3 μM) to investigate their effect on the detection of glucose. The solutions were then separately mixed with C-dots@RGO solution (1 ×, 30 μL). The solutions were then equilibrated at 25 °C for 5 min before being transferred into 96-well microtiter plates prior to PL measurement. A microplate reader (μ-Quant Biotek Instruments, Winooski, VT, USA), with excitation and emission wavelengths of 365 and 440 nm, respectively, was used to record PL of the solutions.

2.6. Detection of glucose in blood and saliva samples

The collected sera were diluted 500-fold with ultrapure water. Aliquots of the diluted samples (30 μL) were added to sodium phosphate buffer (25 mM, pH 9.0, 240 μL) containing GO*x* (1.3 μM) and standard glucose (25–100 μM). The solutions were equilibrated under gentle shaking at 37 °C for 5 min. Subsequently, aliquots (270 μL) of the mixtures were separately mixed with the C-dots@RGO solution (1 ×, 30 μL) and then equilibrated at 25 °C for 5 min prior to PL measurements. As a comparison, the concentrations of glucose in the blood samples were determined using a commercial blood meter (Omnitest EZ) purchased from B. Braun (Mistelweg, Berlin, Germany). The collected saliva samples were diluted 50-fold with ultrapure water. Aliquots of the diluted samples (30 μL) were added to sodium phosphate buffer (25 mM, pH 9.0, 240 μL) containing GO*x* (1.3 μM) and standard glucose (1.3–11.3 μM). The solutions were equilibrated under gentle shaking at 37 °C for 5 min. Subsequently, aliquots (270 μL) of the mixtures were separately mixed with the C-dots@RGO solution (1 ×, 30 μL) and then equilibrated at 25 °C for 5 min prior to PL measurements.

3. Results and discussion

3.1. Sensing strategy

Scheme 1illustrates the sensing strategy for glucose using C-dots@RGO in conjunction with GO*x* that has been used in many glucose biosensors [32], mainly because it is selective to glucose. GO*x* catalyzes the oxidation of glucose to form H_2O_2 as shown in Eq. (1). Through a reaction of glucose with GO*x*, H_2O_2 is generated to induce an increase in the PL of the C-dots@RGO. To support the sensing strategy, different concentrations of standard H_2O_2 solutions were separately added to C-dots@RGO (Fig. S1A), displaying PL increases upon increasing H_2O_2 concentration. The H_2O_2 induced PL enhancement is mainly due to removal of reactive oxygen species (ROS) generated on the surface of C-dots@RGO that caused PL quenching [27,33]. ROS (O_i^-/O_i^{2-}) on the surfaces of C-dots@RGO trapped photogenerated holes to cause recombination of electron–hole pairs through nonradiative means and thus induced PL quenching [34–36]. The reaction between ROS and H_2O_2 is expressed in Eq. (2):

$$GOx+\text{glucose}+O_2 \rightarrow \text{D-glucono-}\delta\text{-lactone}+H_2O_2 \quad (1)$$

$$O_i^-/O_i^{2-}\ (\text{on C-dots@RGO})+H_2O_{2(aq)} \rightarrow \text{C-dots@RGO}+O_{2(g)}+H_2O_{(l)}+e^-/2e^- \quad (2)$$

As ROS is consumed from the surfaces of C-dots@RGO through the reaction with H_2O_2, nonradiative recombination is minimized, leading to the restoration of PL [37]. The concentration of H_2O_2 generated is directly proportional to glucose concentrations, and thus the concentrations of glucose can be determined by measuring the increases in the PL.

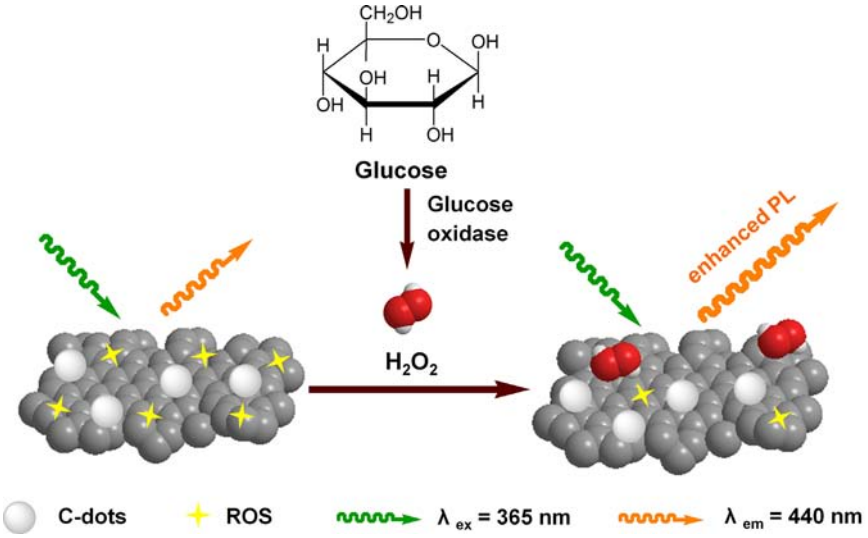

Scheme 1. Schematic representation of the detection of glucose using C-dots@RGO and GO*x*.

3.2. Characterization of C-dots@RGO

The TEM image of C-dots@RGO displayed in Fig. 1A clearly shows layered-structure of RGO and many C-dots (darker spots) on their surfaces. At high temperature (300 °C), RGO and C-dots were separately formed from GO and catechin, in which catechin acted as a reducing agent and a carbon source [27]. The formation of C-dots@RGO was evident as supported by the spectra of Raman, Fourier Transform Infrared, X-Ray Diffraction, and C 1s X-ray photoelectron spectroscopy profiles [27]. Fig. 1B displays the absorption spectrum of C-dots@RGO over the wavelength range from 200 to 600 nm, with a characteristic absorption band at 276 nm that is assigned for the π–π^* transition of C-dots [38]. The PL spectra of C-dots@RGO shown in Fig. 1B reveal the excitation-wavelength dependence characteristics of C-dots, which is due to their various surface states, wide size distribution, and crystal defects [39]. The PL spectra reveal that the maximum emission wavelength is located at 440 nm when excited at a wavelength 365 nm. Thus the two wavelengths were selected for the further study.

3.3. Optimal detection conditions

We investigated the effect of pH values (4.0–11.0) on the detection of H_2O_2 in phosphate solution (20 mM) using C-dots@RGO. Fig. S1B reveals that the optimal pH value was 9.0. At high pH values, the −OH residues on the surface of C-dots dissociate more completely, leading to greater negative density and stability in aqueous solutions as supported by the increased negative zeta potential values upon increasing pH values from pH 4.0 to pH 9.0 (Fig. S2) [40,41]. In addition, C-dots@RGO aqueous solution was stable for at least 60 days when stored at 4 °C. As a result, it is more difficult for the ROS to be adsorbed on the surfaces of C-dots@RGO, mainly due to electrostatic repulsion. The optimal pH for the detection of glucose was also found to be pH 9.0 as shown in Fig. S3A, which is in good agreement with the optimal pH value for the activity of GO*x* [42]. At pH > 9.0, decomposition of H_2O_2 occurred rapidly, leading to PL quenching as a result of generation of more ROS [43]. Fig. S3B reveals that NaCl concentration (up to 350 mM) did not affect the PL of C-dots@RGO in the presence of glucose and GO*x*, showing their great potential for the detection of glucose in biological samples. Fig. S3C shows that the optimal concentration of GO*x* for this assay was 1 μM. Although the reaction rate for the production of H_2O_2 increases upon increasing the concentration of GO*x*, interference from the intrinsic PL of GO*x* became an issue at the GO*x* concentration greater than 1 μM. We further compared the H_2O_2 induced PL enhancement of C-dots@RGO and free C-dots (prepared from catechin). Fig. S4 displays that C-dots@RGO relative to free C-dots provided better sensitivity for H_2O_2, mainly because of greater surface and electron conductivity provided by RGO that allowed faster electron transfer between O_i^-/O_i^{2-} and H_2O_2 on RGO [44,45].

3.4. Selectivity and sensitivity

Under the optimal conditions, the PL intensity increased upon increasing the concentration of glucose, with a linear response (r=0.99) over a concentration range of 600 nM–40 μM (Fig. 2A), in which I_{PL0} and I_{PL} represent the PL intensities of the mixtures in the absence and presence of glucose, respectively. The limit of detection (LOD) for glucose (signal-to-noise ratio=3) is about 230 nM. We have compared the sensitivity of the C-dots@RGO assay with other optical and electrochemical methods (Table 1). The linear glucose concentration range determined using this assay is comparable with those obtained from the reported approaches [6,8,9,15,17,19,21]. Relative to the reported approaches, this assay provides a lower LOD, which allows determination of glucose level in saliva samples. Low matrix interference provided by this assay is another advantage. We also point out that preparation of low-cost C-dots@RGO is straightforward. Without using other enzymes and/or reagents such as horseradish peroxidase or 3,3′,5,5′-tetramethylbenzidine, the cost of the assay using C-dots@RGO is lower. Our approach also allowed reproducible preparation of high-quality C-dots@RGO; their batch-to-batch (n=5) PL intensity varied less than 7%.

We then separately investigated the selectivity of the assay toward glucose (100 μM) over several other carbohydrates (100 μM each), including maltose, lactose, fructose, galactose, and mannose; thiol compounds (10 μM each), including glutathione, cysteine, and homocysteine; and proteins (10 μM each), including BSA and globulin. Fig. 2B displays the selectivity results of C-dots@RGO assay toward glucose in the presence of other interfering species. The results clearly reveal the good selectivity of this approach toward glucose over other tested carbohydrates. For example, the response ratios of glucose over galactose and fructose were 36- and 64-fold, respectively. The activities of a commercial GO*x* for glucose, mannose, lactose, and maltose were 1413, 1095, 92, 665 unit, respectively [46]. We point out that the concentration of glucose in serum and saliva samples is higher than all other carbohydrates by a factor of 100-fold [47–50]. In other words, interference from other carbohydrates in the determination of

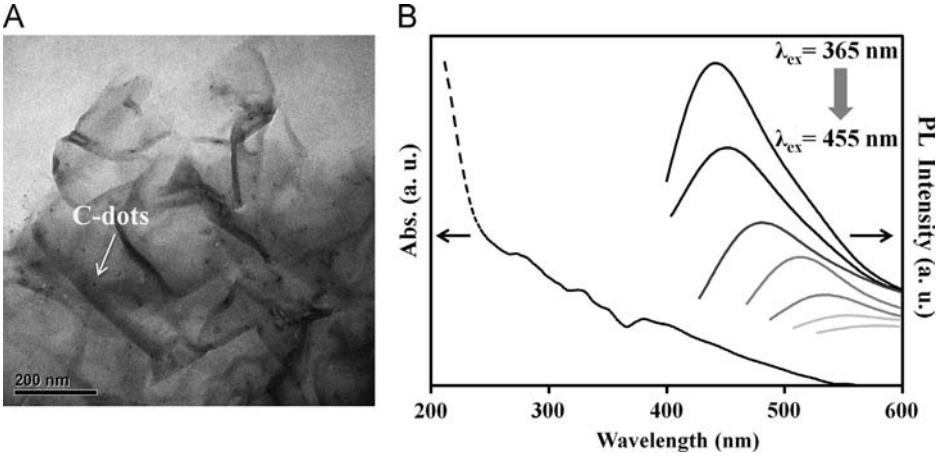

Fig. 1. (A) TEM image and (B) UV–vis absorption spectrum and PL spectra of C-dots@RGO. The excitation wavelength varied from 365 to 455 nm, with 15-nm increments. PL intensities and absorbance are separately plotted in arbitrary units (a. u.). The concentration of C-dots@RGO is 0.1 × (0.2 mg mL^{-1}).

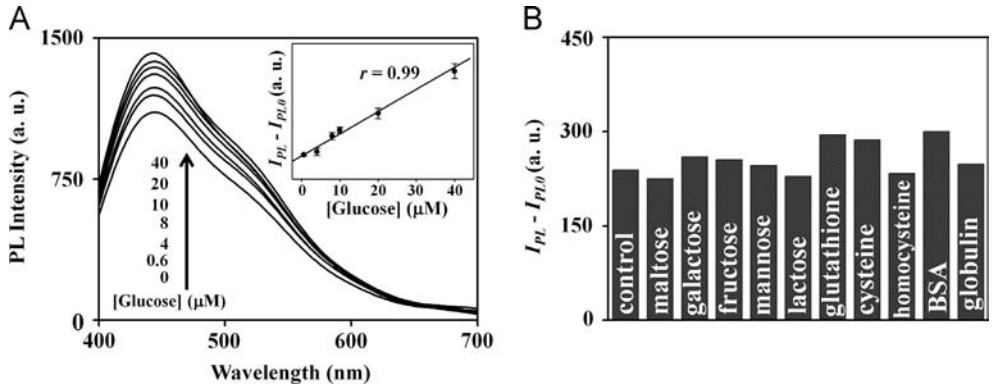

Fig. 2. (A) Sensitivity and (B) selectivity of the assay using C-dots@RGO and GO*x* for the detection of glucose. (A) PL spectra at various glucose concentrations. Inset: linearity of the expression (I_{PL}–I_{PL0}) versus glucose concentration. The concentrations of C-dots@RGO and GO*x* are 0.1 × and 1 μM, respectively. The solutions were prepared in sodium phosphate solution (20 mM, pH 9.0). (B) Selectivity of C-dots@RGO assay towards glucose (100 μM) in the presence of other potential interfering species. The concentrations of the carbohydrates are all 100 μM, and those of thiol compounds and proteins are all 10 μM. 100 μM glucose solution without any interfering species was used as a control. I_{PL0} and I_{PL} are the PL intensities of the solutions in the absence and presence of glucose, respectively. Excitation and emission wavelengths are 365 and 440 nm, respectively.

Table 1
Comparison of various approaches for detection of glucose.

Method	Detection mode	LOD (μM)	Linear range (M)	Ref.
μPADs [a]	Colorimetry	38.1	5.0×10^{-5}–1.0×10^{-3}	[6]
Biosensor	Colorimetry	0.38	1.0×10^{-6}–1.0×10^{-4}	[8]
Biosensor	Colorimetry	2.5	5.0×10^{-6}–5.3×10^{-4}	[17]
Biosensor	Colorimetry	10	2.0×10^{-5}–3.0×10^{-4}	[19]
Biosensor	Fluorescence	1	3.0×10^{-5}–1.0×10^{-3}	[9]
Biosensor	Electrochemiluminescence	0.5	1.0×10^{-6}–1.0×10^{-3}	[15]
Biosensor	Amperometry	6.1	4.0×10^{-5}–2.2×10^{-2}	[21]
Biosensor	Photoluminescence	0.14	1.0×10^{-6}–6.0×10^{-5}	This study

[a] μPADs: Microfluidic paper-based analysis device.

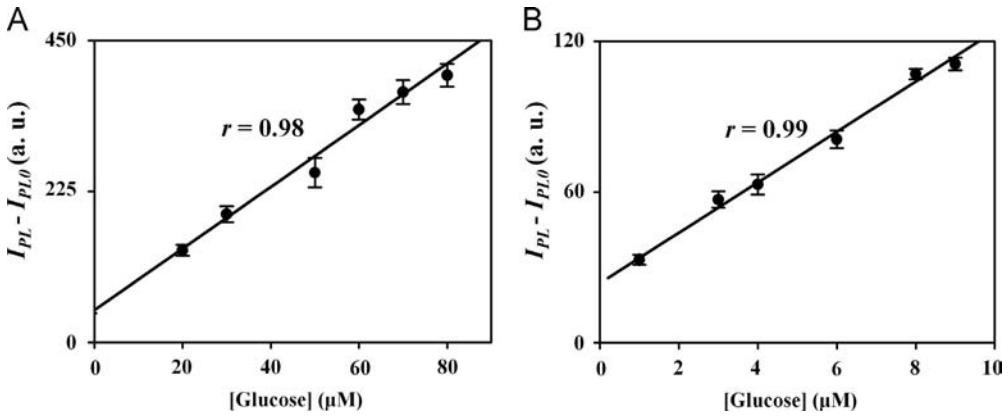

Fig. 3. Analyses of representative (A) serum and (B) saliva samples using C-dots@RGO and GOx. The diluted serum and saliva samples were separately spiked with glucose, with final concentrations in the ranges of 20–80 and 1–9 μM, respectively. Other conditions are the same as those described in Fig. 2.

glucose by our nanosensor can be ignored. Glutathione and cysteine had greater effects than homocysteine on this assay for the determination of glucose, mainly because of their stronger antioxidation strength [51,52]. Their effects on the detection of glucose were also negligible, mainly because their concentrations (< 50 μM) in human serum samples are lower than that of glucose [53]. Globulin and BSA both induced PL enhancement, which also had impacts on the detection of glucose. The PL enhancements of C-dots@RGO are mainly because of reduced surface defects of C-dots through adsorption of these proteins [54]. The PL intensity of C-dots@RGO improved upon increasing BSA concentration from 1–50 μM as depicted in Fig. S5A. The C-dots@RGO has greater response toward glucose in the presence of 10 μM over 1 μM BSA as shown in Fig. S5B. The sensitivity obtained in the presence of 10 μM BSA was higher, mainly because BSA induced PL enhancement. As a result, the LODs for glucose in the presence of 10 μM BSA was 140 nM, which is lower than that (380 nM) in the presence of 1.0 μM BSA. We note that the concentrations of the two most abundant proteins–HSA and globulin—in human serum are 3.4–5.4 g dL^{-1} (507–806 μM) and 2.6–4.6 g dL^{-1} (236–418 μM), respectively [55,56]. Their concentrations in 500-fold diluted blood samples were lower than 10 μM, suggesting that our assay could be applied to the determination of the concentrations of glucose in blood samples. In addition, interference from superoxide, hydroxyl radical, and singlet oxygen can be ignored in the diluted sample, mainly because of their short life times and low concentrations [57].

3.5. Detection of glucose in blood and saliva sample

To test the practicality of this assay, we applied this simple assay for the analyses of blood and saliva samples. In order to minimize the interference of matrices such as HSA, we conducted a standard addition method for the analysis of diluted samples using C-dots@RGO. The PL responses against the concentrations of glucose spiked into representative serum samples were linear ($r=0.98$) in the concentration range of 20–80 μM (Fig. 3A). By using the calibration curve and bringing a dilution factor (500-fold) into calculation, we determined glucose concentration in the serum sample to be 5.1 ± 0.6 mM ($n=3$). Using a commercial blood meter, the concentration of glucose in the same sample was determined to be 5.4 ± 0.3 mM ($n=3$). A *t*-test value of 2.77 was obtained, which is smaller than that (2.92) at a 95% confidence level, revealing that the two approaches did not provide significantly different results. The assay was further applied to determine the concentration of glucose in a representative diluted saliva sample. The PL response against the concentrations of spiked glucose was linear ($r=0.99$) over a range of 1–9 μM (Fig. 3B). By using the calibration curve and bringing a dilution factor (50-fold) into calculation, the glucose concentration was determined to be 117.9 ± 8.1 μM ($n=3$), which is in good agreement with that of the saliva samples (80–300 μM) from healthy people [31,58].

4. Conclusions

We developed a sensitive, selective, and cost-effective approach using C-dots@RGO and GO*x* for the detection of glucose, based on H_2O_2 induced increased PL. Because BSA minimizes ROS quenching of the PL of C-dots@RGO, our assay provides better sensitivity in the presence than absence of 10 μM BSA; LODs are 140 and 230 nM, respectively. Our simple, sensitive, selective, and low-cost assay allows the detection of glucose in blood and saliva samples, revealing its great potential for the analysis of glucose in biological samples. Because the assay is based on H_2O_2 induced PL increases, our assay can also be applied to the detection of various analytes when other enzymes are used; for example, cholesterol can be detected when cholesterol oxidase is used.

Acknowledgment

This study was supported by the National Science Council of Taiwan under Contract NSC 101-2627-M-002-007.

Appendix A. Supporting information

Supplementary data associated with this article can be found in the online version at http://dx.doi.org/10.1016/j.talanta.2013.06.035.

References

[1] J.E. Shaw, R.A. Sicree, P.Z. Zimmet, Diabetes Res. Clin. Pract. 87 (2010) 4–14.
[2] E. Ferrannini, Endocr. Rev. 19 (1998) 477–490.
[3] Y. Xu, P.E. Pehrsson, L. Chen, R. Zhang, W. Zhao, J. Phys. Chem. C 111 (2007) 8638–8643.
[4] X. Chen, S. Dong, Biosens. Bioelectron. 18 (2003) 999–1004.
[5] J. Lee, S.-M. Park, Anal. Chim. Acta 545 (2005) 27–32.
[6] X. Chen, J. Chen, F. Wang, X. Xiang, M. Luo, X. Ji, Z. He, Biosens. Bioelectron. 35 (2012) 363–368.
[7] X. Huang, J. Ren, Trac-Trends Anal. Chem. 40 (2012) 77–89.
[8] P. Roy, Z.-H. Lin, C.-T. Liang, H.-T. Chang, Chem. Commun. 48 (2012) 4079–4081.
[9] Y.-C. Shiang, C.-C. Huang, H.-T. Chang, Chem. Commun. 23 (2009) 3437–3439.
[10] D.L. Williams, A.R. Doig, A. Korosi, Anal. Chem. 42 (1970) 118–121.
[11] L. Coche-Guérente, A. Deronzier, P. Mailley, J.-C. Moutet, Anal. Chim. Acta 289 (1994) 143–153.
[12] H. Wei, E. Wang, Anal. Chem. 80 (2008) 2250–2254.
[13] Z.-F. Zhang, H. Cui, C.-Z. Lai, L.-J. Liu, Anal. Chem. 77 (2005) 3324–3329.
[14] H. Masaki, T. Atsumi, H. Sakurai, Biochem. Biophys. Res. Commun. 206 (1995) 474–479.
[15] B. Haghighi, S. Bozorgzadeh, L. Gorton, Sens. Actuator B-Chem 155 (2011) 577–583.
[16] T. Li, K. Zhu, S. He, X. Xia, S. Liu, Z. Wang, X. Jiang, Analyst 136 (2011) 2893–2896.
[17] Y. Zhang, W. Jia, M. Cui, C. Dong, S. Shuang, Y. Kwan, M.M.F. Choi, Biotechnol. J. 6 (2011) 492–500.
[18] X. Huang, T. Lan, B. Zhang, J. Ren, Analyst 137 (2012) 3659–3666.
[19] B. Malvi, C. Panda, B.B. Dhar, S.S. Gupta, Chem. Commun. 48 (2012) 5289–5291.
[20] L.-M. Lu, H.-B. Li, F. Qu, X.-B. Zhang, G.-L. Shen, R.-Q. Yu, Biosens. Bioelectron. 26 (2011) 3500–3504.
[21] M. Han, S. Liu, J. Bao, Z. Dai, Biosens. Bioelectron. 31 (2012) 151–156.
[22] C.-C. Huang, H.-T. Chang, Chem. Commun. 12 (2007) 1215–1217.
[23] P.-C. Hsu, H.-T. Chang, Chem. Commun. 48 (2012) 3984–3986.
[24] P.-C. Hsu, Z.-Y. Shih, C.-H. Lee, H.-T. Chang, Green Chem. 14 (2012) 917–920.
[25] S.N. Baker, G.A. Baker, Angew. Chem. Int. Ed. 49 (2010) 6726–6744.
[26] Y.-P. Sun, B. Zhou, Y. Lin, W. Wang, K.A.S. Fernando, P. Pathak, M.J. Meziani, B.A. Harruff, X. Wang, H. Wang, P.G. Luo, H. Yang, M.E. Kose, B. Chen, L.M. Veca, S.-Y. Xie, J. Am. Chem. Soc. 128 (2006) 7756–7757.
[27] C.-I. Wang, A.P. Periasamy, H.-T. Chang, Anal. Chem. 85 (2013) 3263–3270.
[28] Y. Liu, D. Yu, C. Zeng, Z. Miao, L. Dai, Langmuir 26 (2010) 6158–6160.
[29] D.B. Sacks, Diabetes Care 34 (2011) 518–523.
[30] K. Wongravee, G.R. Lloyd, C.J. Silwood, M. Grootveld, R.G. Brereton, Anal. Chem. 82 (2009) 628–638.
[31] C. Jurysta, N. Bulur, B. Oguzhan, I. Satman, T.M. Yilmaz, W.J. Malaisse, A. Sener, J. Biomed. Biotechnol. 2009 (2009) 430426.
[32] S.B. Bankar, M.V. Bule, R.S. Singhal, L. Ananthanarayan, Biotechnol. Adv. 27 (2009) 489–501.
[33] Y. Zhang, S.F. Ali, E. Dervishi, Y. Xu, Z. Li, D. Casciano, A.S. Biris, ACS Nano 4 (2010) 3181–3186.
[34] G. Dukovic, B.E. White, Z. Zhou, F. Wang, S. Jockusch, M.L. Steigerwald, T.F. Heinz, R.A. Friesner, N.J. Turro, L.E. Brus, J. Am. Chem. Soc. 126 (2004) 15269–15276.
[35] N. Haralampus-Grynaviski, C. Ransom, T. Ye, M. Rôżanowska, M. Wrona, T. Sarna, J.D. Simon, J. Am. Chem. Soc. 124 (2002) 3461–3468.
[36] E. Mihokova, M. Nikl, P. Bohacek, V. Babin, A. Krasnikov, A. Stolovich, S. Zazubovich, A. Vedda, M. Martini, T. Grabowski, J. Lumin. 102–103 (2003) 618–622.
[37] W.-Y. Su, J.-S. Huang, C.-F. Lin, J. Cryst. Growth 310 (2008) 2806–2809.
[38] Z. Zhang, J. Hao, J. Zhang, B. Zhang, J. Tang, RSC Adv. 2 (2012) 8599–8601.
[39] Y.-M. Long, C.-H. Zhou, Z.-L. Zhang, Z.-Q. Tian, L. Bao, Y. Lin, D.-W. Pang, J. Mater. Chem. 22 (2012) 5917–5920.
[40] S.-T. Yang, S. Chen, Y. Chang, A. Cao, Y. Liu, H. Wang, J. Colloid Interface Sci. 359 (2011) 24–29.
[41] F. Lin, W.N. He, X.Q. Guo, Adv. Mater. Res. (2011) 1319–1322.
[42] C. Marquette, D. Thomas, A. Degiuli, L. Blum, Anal. Bioanal. Chem. 377 (2003) 922–928.
[43] Z. Qiang, J.-H. Chang, C.-P. Huang, Water Res. 36 (2002) 85–94.
[44] B. Hu, R. Quhe, C. Chen, F. Zhuge, X. Zhu, S. Peng, X. Chen, L. Pan, Y. Wu, W. Zheng, Q. Yan, J. Lu, R.-W. Li, J. Mater. Chem. 22 (2012) 16422–16430.
[45] A. Iwase, Y.H. Ng, Y. Ishiguro, A. Kudo, R. Amal, J. Am. Chem. Soc. 133 (2011) 11054–11057.
[46] M. Kobayashi, H. Nishara, S. Kobayashi, J. Appl. Glycosci 46 (1999) 1–7.
[47] A.M. Horgan, A.J. Marshall, S.J. Kew, K.E.S. Dean, C.D. Creasey, S. Kabilan, Biosens. Bioelectron. 21 (2006) 1838–1845.
[48] T. Kawasaki, N. Ogata, H. Akanuma, T. Sakai, H. Watanabe, K. Ichiyanagi, T. Yamanouchi, Metabolism 53 (2004) 583–588.
[49] T. Kawasaki, H. Akanuma, T. Yamanouchi, Diabetes Care 25 (2002) 353–357.
[50] O.M. Pitkänen, H. Vanhanen, E. Pitkänen, Scand. J. Clin. Lab. Invest. 59 (1999) 607–612.
[51] A. Pompella, A. Visvikis, A. Paolicchi, V.D. Tata, A.F. Casini, Biochem. Pharmacol. 66 (2003) 1499–1503.
[52] R.J. Elias, D.J. McClements, E.A. Decker, J. Agric. Food Chem. 53 (2005) 10248–10253.
[53] C. Carru, A. Zinellu, S. Sotgia, R. Serra, M.F. Usai, G.F. Pintus, G.M. Pes, L. Deiana, Biomed. Chromatogr. 18 (2004) 360–366.
[54] J.-M. Liu, L.-P. Lin, X.-X. Wang, S.-Q. Lin, W.-L. Cai, L.-H. Zhang, Z.-Y. Zheng, Analyst 137 (2012) 2637–2642.
[55] G.P. Chrousos, A. Vingerhoeds, D. Brandon, C. Eil, M. Pugeat, M. DeVroede, D.L. Loriaux, M.B. Lipsett, J. Clin. Invest. 69 (1982) 1261–1269.
[56] B.M. Dworkin, W.S. Rosenthal, G.P. Wormser, L. Weiss, J. Parenter. Enter. Nutr. 10 (1986) 405–407.
[57] T. Devasagayam, J. Tilak, K. Boloor, K.S. Sane, S.S. Ghaskadbi, R. Lele, J. Assoc, Phys. India 52 (2004) 794–804.
[58] M.S. Soares, M.M. Batista-Filho, M.J. Pimentel, I.A. Passos, E. Chimenos-Kustner, Med. Oral Patol. Oral Cir. Bucal 14 (2009) e510–e513.